



HAL
open science

Quantifying the release of climate-active gases by large meteorite impacts with a case study of Chicxulub.

Natalia Artemieva, Joanna Morgan, S.P.S. Gulick, E. Chenot, G.L. Christeson, P. Claeys, C.S. Cockell, M.J.L. Coolen, L. Ferrière, C. Gebhardt, et al.

► To cite this version:

Natalia Artemieva, Joanna Morgan, S.P.S. Gulick, E. Chenot, G.L. Christeson, et al.. Quantifying the release of climate-active gases by large meteorite impacts with a case study of Chicxulub.. *Geophysical Research Letters*, 2017, 44 (20), pp.10180-10188. 10.1002/2017GL074879 . hal-01639659

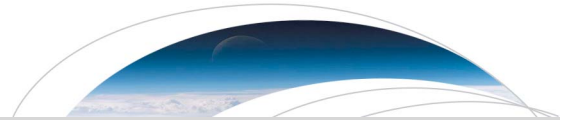
HAL Id: hal-01639659

<https://hal.science/hal-01639659>

Submitted on 13 Apr 2018

HAL is a multi-disciplinary open access archive for the deposit and dissemination of scientific research documents, whether they are published or not. The documents may come from teaching and research institutions in France or abroad, or from public or private research centers.

L'archive ouverte pluridisciplinaire **HAL**, est destinée au dépôt et à la diffusion de documents scientifiques de niveau recherche, publiés ou non, émanant des établissements d'enseignement et de recherche français ou étrangers, des laboratoires publics ou privés.



RESEARCH LETTER

10.1002/2017GL074879

Key Points:

- We use a hydrocode to model shock pressures, ejection velocities, and amount of gases released from sedimentary rocks after large impacts
- We use new constraints on impact angle and target composition to improve estimates of the gases released by the Chicxulub impact
- We investigate the effects of sediment porosity, submergence under water, and uncertainties in devolatilization pressures on our estimates

Supporting Information:

- Supporting Information S1

Correspondence to:

N. Artemieva,
artemeva@psi.edu

Citation:

Artemieva, N., Morgan, J., & Expedition 364 Science Party (2017). Quantifying the release of climate-active gases by large meteorite impacts with a case study of Chicxulub. *Geophysical Research Letters*, 44, 10, 180–10,188. <https://doi.org/10.1002/2017GL074879>

Received 13 JUL 2017

Accepted 18 SEP 2017

Published online 30 OCT 2017

Quantifying the Release of Climate-Active Gases by Large Meteorite Impacts With a Case Study of Chicxulub

Natalia Artemieva¹ , Joanna Morgan² , and Expedition 364 Science Party³

¹Planetary Science Institute, Tucson, AZ, USA, ²Department of Earth Science and Engineering, Imperial College London, London, UK, ³See section A2

Abstract Potentially hazardous asteroids and comets have hit Earth throughout its history, with catastrophic consequences in the case of the Chicxulub impact. Here we reexamine one of the mechanisms that allow an impact to have a global effect—the release of climate-active gases from sedimentary rocks. We use the SOVA hydrocode and model ejected materials for a sufficient time after impact to quantify the volume of gases that reach high enough altitudes (> 25 km) to have global consequences. We vary impact angle, sediment thickness and porosity, water depth, and shock pressure for devolatilization and present the results in a dimensionless form so that the released gases can be estimated for any impact into a sedimentary target. Using new constraints on the Chicxulub impact angle and target composition, we estimate that 325 ± 130 Gt of sulfur and 425 ± 160 Gt CO₂ were ejected and produced severe changes to the global climate.

Plain language Summary Potentially hazardous asteroids and comets have hit Earth throughout its history, with catastrophic consequences in the case of the Chicxulub impact 66 Myr ago. Here we reexamine one of the mechanisms that allow an impact to have a global effect—the release of climate-active gases from terrestrial sedimentary rocks after the high-velocity impact. We estimate that 325 ± 130 Gt of sulfur and 425 ± 160 Gt CO₂ were ejected into the atmosphere at velocities > 1 km/s. These numbers have to be used in global climate models to quantify possible changes of solar irradiation, surface temperature, and duration of stressful conditions for biota.

1. Introduction

The hazardous effects of impacts became a topic of great interest following the realization that the Earth was hit by a large asteroid or comet ~ 66 Ma and that this impact coincided with the K-Pg mass extinction (Alvarez et al., 1980). It is obvious why a large impact might be locally devastating, with the emission of high levels of thermal radiation from the impact plume, the generation of hurricane-force winds, and potential to cause tsunamis and landslides (Bourgeois et al., 1988; Bralower et al., 1998; Collins et al., 2005; Ward & Asphaug, 2000). For an impact to cause a mass extinction it must have global consequences. Proposed kill mechanisms for the K-Pg mass extinction include the following: short-term cooling and darkness produced by dust, soot, and sulfur in the atmosphere (Alvarez et al., 1980; Brett, 1992; Pierazzo et al., 1998; Sigurdsson et al., 1992; Toon et al., 1982); long-term warming from the release of massive volumes of CO₂ (O'Keefe & Ahrens, 1989; Pope et al., 1994); ocean acidification (e.g., D'Hondt et al., 1994); and global firestorms ignited when ejecta heats up as it reenters the Earth's atmosphere and emits thermal radiation (Melosh et al., 1990; Morgan et al., 2013; Wolbach et al., 1985).

The cause of the K-Pg mass extinction remains a matter of some debate, but the environmental effects of climatically active gases released from sedimentary rocks at the Chicxulub impact site is still one of the widely favored kill mechanisms (Brugger et al., 2017; Schulte et al., 2010). When an impact-induced shock wave of sufficiently high pressure passes through sedimentary rocks, they decompose and form part of the expanding impact plume. For Chicxulub, where seawater, porous carbonates, and evaporites formed the upper portion of the target, this process led to the injection of CO₂, S-bearing gases, and water vapor into the atmosphere. In these circumstances sulfur rapidly forms an aerosol, which backscatters and absorbs solar radiation causing rapid cooling at the Earth's surface, while the addition of CO₂ contributes to longer-term warming (Kring, 2007). Early estimates of the released gases (e.g., Sigurdsson et al., 1992; Takata & Ahrens, 1994)

were hampered by uncertainty in the target rocks at the impact site and inaccurate equations of state; these issues were partially addressed by Pierazzo et al. (1998), who determined that 40–560 Gt of sulfur, 350–3,500 Gt of CO₂, and 200–1,400 Gt of water vapor were released into the atmosphere. The large range of estimated values arises, in part, due to uncertainty in the angle of impact and the relative volumes of carbonates and evaporites in the target rocks. Due to computational cost, this and all other previous models (e.g., Ivanov et al., 1996) only modeled the first few seconds of a vertical impact, meaning that they were able to estimate the amount of highly shocked sedimentary rock but unable to quantify the volume of gases ejected to a sufficient height in the atmosphere (>25 km) to cause a global effect (Toon et al., 1997).

Here we revisit these calculations with the goal of improving estimates of the release of climate-active gases during large impacts in general and the Chicxulub impact in particular. Released gases are important inputs to global climate models (GCM), which are used to simulate the environmental changes over the months to hundreds of years following an impact (Pierazzo et al., 2003) and suggest that surface temperatures were reduced by > 20°C and took over 30 years to recover following the Chicxulub impact (Brugger et al., 2017). We use a more advanced hydrocode (Artemieva, 2017) and recent improvements in the equations of state (EOS) (Melosh, 2007) and run the simulations for at least 15–30 s (depending on impact scenario) to ensure that all ejecta with velocities >1 km/s has exited the growing crater. This approach more accurately estimates the total mass ejected to >25 km altitude for a range of different impact scenarios. For Chicxulub, we use new constraints on impact angle (Collins et al., 2017) and target composition (Belza et al., 2012; Kenkmann et al., 2004) to estimate the gases released by this impact.

2. Method

We use the multiphase hydrocode SOVA (Shuvalov, 1999), which is a 3-D Eulerian code that models multidimensional, multimaterial, large deformation, strong shock wave physics (see section A3). We use SOVA for several reasons, but principally because, unlike the widely used CTH and iSALE hydrocodes, it has the capability to simulate the dynamics of different materials within the impact plume. Due to improvements in computational power, we are able to model oblique impacts and run our simulations for longer time periods and with millions of tracer particles (as opposed to a thousand in previous studies) to more accurately capture properties such as maximum shock compression, gas/vapor/melt production, and ejecta velocity.

A major uncertainty in calculations of gases released from sedimentary rocks is the assignment of shock pressures for incipient and complete vaporization (Bell, 2016). Experiments on rock samples in containers are considered to overestimate shock pressures for degassing due to the lack of free space (Langenhorst & Deutsch, 2012) and lower energy gain during decompression (Prescher et al., 2011). Results from individual laboratory experiments and various theoretical studies indicate that calcite decomposes to CO₂ and CaO at pressures of between 10 and 100 GPa (Kotra et al., 1983; Lange & Ahrens, 1986; Tyburczy & Ahrens, 1986; Yang et al., 1996). Although rocks with dry porosity decompose at lower shock pressures than nonporous rocks (Ivanov & Deutsch, 2002; Martinez et al., 1995), rocks with wet porosity appear to show similar behavior to nonporous rocks (Güldemeister et al., 2013; Kowitz et al., 2016). For this reason, we have assumed that both the porous (water-saturated) and nonporous calcite decompose at the same shock pressure, with incipient decomposition starting at 60 GPa and full decomposition at shock pressures of 100 GPa, in accordance with shock experiments, numerical simulations, and thermodynamic calculations by Yang et al. (1996). In the supporting information, we include additional estimates with different shock devolatilization pressures in order to investigate how uncertainties in the critical pressures for decomposition of calcite affect our estimates of released gases.

For our compilation of results, we use a carbonate target (analytical equations of state, ANEOS, for calcite) with 0 and 20% wet porosity (mass fraction of calcite 0.91), a projectile of 10 km in diameter traveling at 18 km/s, and impact angles of 15, 30, 45, 60, and 90° to the horizontal. We select a resolution of 20 cells per projectile radius, a density of 2.6 g/cm³ for the projectile and nonporous target, and 2.28 g/cm³ for the porous target. For our simulations using porous calcite, we assume that pores are filled with water (mixed ANEOS as described in Pierazzo et al., 2005). For all the results presented here, we only include materials that are ejected from the impact site with velocities higher than 1 km/s, because ejecta with lower velocities will not reach high altitudes and, hence, cannot be redistributed globally. For the case study of Chicxulub, we investigate the addition of anhydrite of zero porosity within the target. According to laboratory

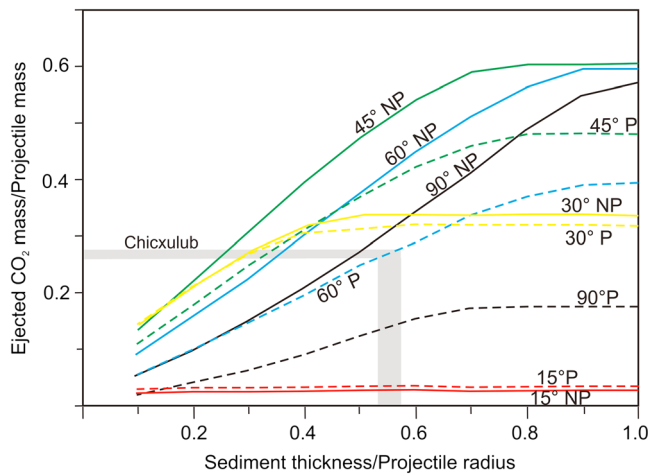


Figure 1. Mass of CO₂ ejected to high altitudes (> 25 km), relative to the mass of the projectile (Y axis) for impact angles of 15 (red), 30 (yellow), 45 (green), 60 (blue), and 90° (black). Solid and dashed lines are for nonporous (NP) and porous (P) calcite, respectively. The X axis is carbonate thickness divided by projectile radius. Assuming an impact angle of 60° and projectile radius of 6.1 km for Chicxulub, the colored gray zone shows the range covered by carbonate thicknesses of between 3.3 km and 3.5 km, which correspond to X axis values of 0.54 and 0.57, respectively.

1.5 km diameter projectile traveling at 18 km/s that hit the Earth at a ~ 30° impact angle (Artemieva et al., 2013). Using these values and a density of 2.6 g/cm³, the projectile mass is 4.6 Gt. The uppermost target rocks in the area are thought to include a ~ 300 m thick porous water-saturated carbonate, which corresponds to a ratio on the X axis (thickness of sedimentary rock/projectile radius) of 0.4, leading to a degassed CO₂ mass of ~1.3 Gt (~0.29 times the projectile mass), and solid sediment mass of 19 Gt.

To use the results shown in Figures 1 and 2 for other impacts on Earth, the projectile diameter (D_{pr}) should be scaled so that it reproduces the diameter of the observed transient cavity (D_{tc}) for an impact velocity of 18 km/s using the scaling law from Holsapple and Housen (2007):

$$D_{tc} = 18^{0.44} D_{pr}^{0.78}$$

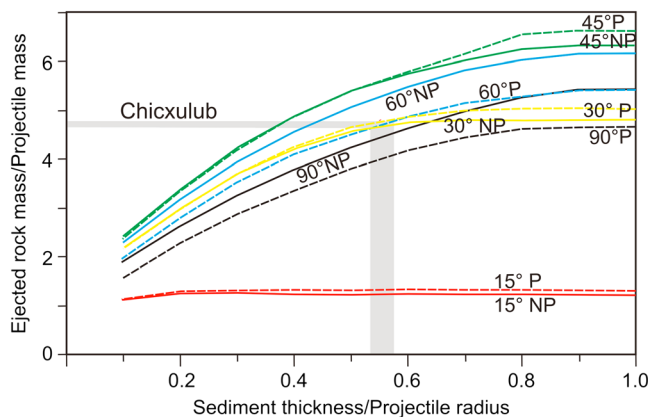


Figure 2. Mass of solid calcite ejected to high altitudes (> 25 km), relative to the mass of the projectile (Y axis) for impact angles of 15 (red), 30 (yellow), 45 (green), 60 (blue), and 90° (black). Solid and dashed lines are for nonporous (NP) and porous (P) calcite, respectively. The X axis is carbonate thickness divided by projectile radius. Assuming an impact angle of 60° and projectile radius of 6.1 km for Chicxulub, the colored gray zone shows the range covered by carbonate thicknesses of between 3.3 km and 3.5 km, which correspond to X axis values of 0.54 and 0.57, respectively.

experiments and theoretical studies, anhydrite degasses between 30 and 180 GPa (Badjukov et al., 1995; Gupta et al., 2001; Ivanov et al., 1996; Yang et al., 1996). Here we assume incipient decomposition of anhydrite at 30 GPa and full decomposition at 120 GPa, in accordance with thermodynamic and experimental data (Gupta et al., 2001; Prescher et al., 2011). We do not use anhydrite EOS for our mixed calcite/anhydrite target (Pierazzo et al., 1998) as the anhydrite EOS requires additional adjustment before it can be incorporated into the new version of the ANEOS package (Melosh, 2007) and the SOVA code is not able to deal with four different materials in one computational cell. We also examine the effect of submerging the sedimentary sequence under water, as was the case for the Chicxulub impact.

3. Results

The mass of CO₂ generated by the decomposition of porous (P) and nonporous (NP) calcite and ejected to >25 km altitude is shown in Figure 1 and the mass of calcite ejected as a solid in Figure 2. The results are presented in dimensionless form so that they can be used to calculate the volumes of gases (Figure 1) and solid calcite (Figure 2) released from carbonate sequences of different thicknesses and for different impactor sizes. For example, it has been suggested that the 26 km diameter Ries crater could have been formed by a

1.5 km diameter projectile traveling at 18 km/s that hit the Earth at a ~ 30° impact angle (Artemieva et al., 2013). Using these values and a density of 2.6 g/cm³, the projectile mass is 4.6 Gt. The uppermost target rocks in the area are thought to include a ~ 300 m thick porous water-saturated carbonate, which corresponds to a ratio on the X axis (thickness of sedimentary rock/projectile radius) of 0.4, leading to a degassed CO₂ mass of ~1.3 Gt (~0.29 times the projectile mass), and solid sediment mass of 19 Gt.

To use the results shown in Figures 1 and 2 for other impacts on Earth, the projectile diameter (D_{pr}) should be scaled so that it reproduces the diameter of the observed transient cavity (D_{tc}) for an impact velocity of 18 km/s using the scaling law from Holsapple and Housen (2007):

Impact angles of between 30° and 60° (50% of all impacts occur in this interval) are more effective at producing gas, and this occurs because near-vertical impacts produce less high-velocity ejecta whereas more oblique impacts produce smaller volumes of highly shocked materials (Figure 1 and Table S1). We note, however, that a 90° impact into a thick nonporous sedimentary sequence releases a surprising amount of gas. Figures 1 and 2 show that the total mass of CO₂ and solid calcite released is generally lower for the porous calcite than the nonporous, which is expected given that 9% of the calcite mass is replaced with water. However, the dependence of ejecta on porosity is quite complex and does not just lead to a simple reduction by a factor of 0.91 in released gases. At highly oblique impact angles the ratio of degassed sediments in porous and nonporous cases is 1.36 (i.e., a factor of 1.5 larger than expected), and for vertical impacts the ratio is only 0.44 (a factor of 2 smaller than expected) (Table S2). For solid ejecta, the dependence on impact angle is smoother: the ratio of solid sediments released from porous and nonporous calcite is 1.1 for a 15° impact and then approaches the expected value of ~0.9 at impact angles of >45°.

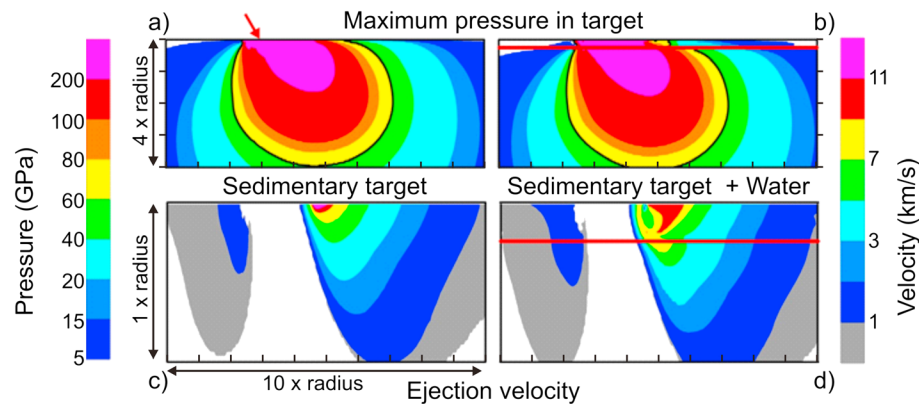


Figure 3. Maximum pressure in the plane of symmetry for a 60° impact into (a) sedimentary target and (b) sedimentary target covered by water. X and Y axes are horizontal distance and depth and correspond to 10 times and 4 times projectile radius, respectively. Red arrow shows impact point, and red line shows water depth which is one fourth of the projectile radius. (c and d) Ejection velocity of target materials for Figures 3a and 3b; X and Y axes are 10 times and 1 times projectile radius, respectively.

Sedimentary sequences close to continental margins are often submerged. Figure 3 shows the results for a thick nonporous sedimentary target without a water layer (Figures 3a and 3c) and submerged in water, where the water has a thickness equal to one fourth of the projectile radius (Figures 3b with 3d). These plots show that the addition of a water layer leads to minimal changes in maximum shock pressure (compare Figures 3a and 3b) and ejection velocity (compare Figures 3c with 3d) with depth. The total amount of sedimentary ejecta is lower by ~ 20 to 35% for a 60° and 30° impact into water, respectively (see column 6 in Table S1), and the amount of decomposed high-velocity sedimentary rocks decreases by 10–30% (see column 3 in Table S1). The other notable difference is that the addition of a water layer leads to the ejection of water, steam, and sea salt to high altitudes. Water is vaporized between pressures of 4 and 10 GPa, and, for the case shown in Figure 3d, the mass of ejected steam and water is ~ 0.8 and 0.67 of the projectile mass, respectively.

4. Chicxulub

Recent IODP-ICDP drilling of the peak ring of the Chicxulub impact crater (Morgan et al., 2016) along with geophysical data have been used to ground truth 3-D numerical simulations of crater formation (Collins et al., 2017). Collins et al. (2017) estimate that the angle of impact at Chicxulub was $\sim 60^\circ$ with a downrange direction to the southwest. We scale the size of the projectile so that with an impact velocity of 18 km/s, it produces a crater with the correctly sized transient cavity (Artemieva & Morgan, 2009), which gives a projectile diameter of 12.2 km (Table S2) and a projectile mass of 2,500 Gt (density = 2.6 g/cm^3). Our numerical simulations indicate that the sedimentary rocks degassed by this impact would have been located in the downrange direction, between 180° and 270° from the crater center. Using offshore seismic data, the sedimentary sequence to the west of the crater center is estimated to be 3.8 ± 0.2 km thick (Bell et al., 2004). No nearby onshore wells to the south of the crater reach crystalline basement, and the sedimentary rocks in the deepest well, Y-2, are 2.8 km thick (López-Ramos, 1975; Rebolledo-Vieyra & Urrutia-Fucugauchi, 2004); hence, their total thickness in this direction is likely to be greater than 2.8 km. In addition, the sedimentary sequence thickens from onshore to offshore and from east to west along reflection profile, Chicx-A/A1, closest to the Yucatán coastline (Morgan & Warner, 1999). Given these considerations, we use a value of 3.3–3.5 km for sedimentary thickness in the southwest portion of the crater, which corresponds to X axis values of between 0.54 and 0.57 in Figures 1 and 2.

Using Figure 1, for a 60° impact angle into a sedimentary target composed of 50% carbonate and 50% anhydrite target (one of the proposed scenarios in Pierazzo et al., 1998) in which the two lithologies are equally distributed, 330 Gt of CO_2 and 400 Gt of S are ejected to altitudes greater than 25 km. The angle of impact is not likely to be exactly 60° , however, and if we assume that it is $60 \pm 10^\circ$, then we can use Figure 1 to place error bars on our estimates, which gives 330 ± 60 Gt CO_2 and 400 ± 60 Gt S. Note that as we vary the impact angle the projectile size varies respectively (see column 1 in Table S2), which means that the X axis values also change. The distribution of anhydrite within the target is also important, and data from the Yaxcopoil-1 drill

Table 1
The Role of Different Factors in CO₂ Production

	Pierazzo et al. (1998) (P98)	This work (A and M)		Effect on net production
Pressure for devolatilization (GPa)	20	60 (Incipient degassing)	100 (Complete degassing)	P98 > A and M
Assumed recombination	31%	Not accounted for		P98 < A and M
Ejection from the crater	Not accounted for	Only includes material ejected at >1 km/s		P98 > A and M
Impact obliquity	Vertical only	15–90° (Max. between 30–60°)		P98 < A and M

Note. P98 is Pierazzo et al. (1998), and A and M are our new calculations.

hole (which is in the southwest direction and just outside the excavation cavity) indicate that the ~600 m thick sedimentary section is late Albian to Campanian in age (Belza et al., 2012) of which ~ 27% is anhydrite (Kenkmann et al., 2004). To the south and southwest of the crater the lower half of the sedimentary sequence is lower Cretaceous in age and ~60% anhydrite (López-Ramos, 1975; Rebolledo-Vieyra & Urrutia-Fucugauchi, 2006). Using the assumption that the upper half of sedimentary sequence is 75% calcite and 25% anhydrite and the lower half is 60% anhydrite and 40% calcite, the ejected masses become 425 ± 60 Gt CO₂ and 325 ± 60 Gt S (Table S3).

At the time of the impact, there was probably a fairly shallow sea covering the northern half of the Yucatán peninsula, but water depths may have been up to 1.5 km deep to the northeast of the point of impact (Gulick et al., 2008), which corresponds to the water thickness (one fourth of the projectile radius) shown in Figures 3b and 3d. We note that if the downrange direction is to the southwest, however, the high-velocity ejecta originate mainly from the target in this direction, which suggests that the effect of deep water in the northeast direction may have been quite minor for the Chicxulub impact.

5. Discussion

The lack of a reliable EOS for anhydrite, as well as uncertainties in devolatilization pressures for calcite and anhydrite, remain a potential source of error in our estimates. Given this, we also ran simulations using pressures of 40 GPa and 80 GPa for incipient degassing and 80 and 120 GPa for complete decomposition of calcite, so that our results can be reassessed should better constraints arise in the future (columns 2–4 in Table S1). For our Chicxulub calculations, changing decomposition pressures by ±20 GPa changes our estimates of released gases by ±35%. If we assume that there is a ± 35% uncertainty in our calculations for both calcite and anhydrite and combine this with the ±60 Gt error due to uncertainty in impact angle, we get values of 425 ± 160 Gt CO₂ and 325 ± 130 Gt S. Also, we note that gypsum produces less sulfur than anhydrite (Table S3), which needs to be taken into account in any future estimates of released climatic gases, should better constraints on target rock composition become available. For all three scenarios, the total amount of ejecta with velocity > 1 km/s remains constant (column 6 in Table S1), and the relative mass of ejected gas versus solid sediment decreases as the critical shock pressures are increased (columns 2–4 in Table S1).

Surprisingly, our results for the Chicxulub impact are comparable to previous estimates by Ivanov et al. (1996) and Pierazzo et al. (1998) (Table S4) and significantly less than Sigurdsson et al. (1992) and Takata and Ahrens (1994). Various factors influence the production of climate-active gases presented here, with some leading to an increase and others a decrease in comparison to previous calculations (see Table 1). All previous calculations assumed lower decomposition pressures for porous calcite (20–30 GPa), which recent research suggests may be incorrect when the pore spaces are filled with water (Güldemeister et al., 2013; Kowitz et al., 2016). We also use different decomposition pressures for anhydrite, based on research published after these earlier calculations were made (Gupta et al., 2001; Prescher et al., 2011). On the other hand, Pierazzo et al. (1998) assumed that ~31% of the ejected CO₂ would be removed early on within the expanding impact plume due to back reactions and thus would not contribute to the global inventory (Table 1). While we recognize that these back reactions do occur and are important, they are not included in our calculations as they are difficult to quantify. We do consider that it is important to ensure that the gases are ejected from the crater at sufficient velocities to reach high altitudes, whereas previous calculations only ran for a few seconds in order to determine shock pressures and then assumed all gases released by shock devolatilization would contribute to the global inventory. Our estimates show that in the case of a thick sedimentary cover (thickness

larger than the projectile radius), only 6–20% (depending on impact angle and porosity) of the highly shocked sediments ($P > 60$ GPa) are ejected with velocities of >1 km/s (compare columns 3 and 7 in Table S1). The remaining shocked materials are either ejected with lower velocity and, hence, stay in the crater vicinity (both CO_2 and SO_x are heavier than atmospheric gases) or stay within the crater and form part of the melt pool and/or suevitic layer. In the Chicxulub case, with a sediment thickness that is equal to 0.54–0.57 of the projectile radius, the effect is smaller: approximately 50% of the sedimentary rocks shocked >60 GPa reach altitudes of >25 km. Finally, impact obliquity has an important effect on released gases with maximum gas production for impact angles of 30–60° (Figure 1).

Another important output from our calculations is the mass of solid sediment ejected to high altitudes (Figure 2), which for Chicxulub corresponds to $\sim 12,000$ Gt ($4.8 \times$ projectile mass). This is consistent with the observation of fine-grained shocked and unshocked carbonate and dolomite clasts in the upper layer of the K-Pg boundary at the Demerara Rise, where they are coincident with shocked tectosilicates (Schulte et al., 2009). The abundance of sedimentary clasts at this location led the authors to conclude that they are a much more common component of Chicxulub ejecta than previously thought. In addition, Schulte et al. (2009) interpret some of the morphologic features (fluidal-shaped micrometer-sized pores) in these clasts as evidence of their formation within the high-temperature impact plume. We propose an alternative explanation, that these high-temperature features may also have been formed when the clasts were heated during atmospheric reentry. This is of particular interest here as it would mean that additional climatic gases were released during the reentry of solid sedimentary material. Future 3-D simulations of the transport of ejecta around the globe will be performed to investigate this further.

6. Conclusions

Our calculations of released gases from sedimentary rocks in general and Chicxulub in particular are more realistic and, thus, improve on previous models because they use a more advanced 3-D hydrocode (Artemieva, 2017) and take into account the following: (1) an updated EOS (Melosh, 2007); (2) the velocity of the ejected gases and ensure that they reach high enough altitudes to have a global effect; (3) improved knowledge of the thickness and composition of the Chicxulub target from new offshore seismic data (Bell et al., 2004) and well data from Yaxcopoil-1 (Kenkmann et al., 2004); and (4) new constraints on the Chicxulub impact angle and direction (Collins et al., 2017). These new estimates of released climatic gases are important inputs to GCM for models of temperatures at the Earth's surface and within the ocean after large impacts (e.g., Brugger et al., 2017) and for quantifying ocean acidification (e.g., D'Hondt et al., 1994). Our estimate of 325 ± 130 Gt of sulfur released is larger than the value used by Brugger et al. (2017) in their GCM, whereas our estimate of 425 ± 160 Gt of CO_2 is smaller than their input. This suggests that surface temperatures were likely to have been significantly reduced for several years and ocean temperatures affected for hundreds of years after the Chicxulub impact.

Appendix A

A1. Author Contribution

N. A. performed all the SOVA hydrocode simulations. J. M. provided new data for the Chicxulub impact site, drafted the figures, and coordinated the preparation of the manuscript. Expedition 364 scientists participated in discussions of the results and edited drafts.

A2. Additional Expedition 364 Scientists (<http://www.ecord.org/expedition364/participants/>)

S. P. S. Gulick¹, E. Chenot², G. L. Christeson¹, P. Claeys³, C. S. Cockell⁴, M. J. L. Coolen⁵, L. Ferrière⁶, C. Gebhardt⁷, K. Goto⁸, S. Green⁹, H. Jones¹⁰, D. A. Kring¹¹, J. Lofi¹², C. M. Lowery¹, R. Ocampo-Torres¹³, L. Perez-Cruz¹⁴, A. E. Pickersgill^{15,16}, M. Poelchau¹⁷, A. S. P. Rae¹⁸, C. Rasmussen¹⁹, M. Rebolledo-Vieyra²⁰, U. Riller²¹, H. Sato²², J. Smit²³, S. M. Tikoo²⁴, N. Tomioka²⁵, J. Urrutia-Fucugauchi¹⁴, M. T. Whalen²⁶, A. Wittmann²⁷, L. Xiao²⁸, K. E. Yamaguchi^{29,30}, W. Zylberman^{31,32}, and third party scientists G. S. Collins¹⁸ and T. J. Bralower¹⁰.

¹Institute for Geophysics and Department of Geological Sciences, Jackson School of Geosciences, University of Texas at Austin, Austin, TX, USA, ²Biogéosciences Laboratory, Université de Bourgogne-Franche Comté, Dijon, France, ³Analytical, Environmental and Geo-Chemistry, Vrije Universiteit Brussel, Brussels, Belgium, ⁴Centre for Astrobiology, School of Physics and Astronomy, University of Edinburgh, Edinburgh, UK,

⁵Department of Chemistry, WA-Organic and Isotope Geochemistry Centre, Curtin University, Perth, Western Australia, Australia, ⁶Natural History Museum, Vienna, Austria, ⁷Alfred Wegener Institute Helmholtz Centre of Polar and Marine Research, Bremerhaven, Germany, ⁸International Research Institute of Disaster Science, Tohoku University, Sendai, Japan, ⁹British Geological Survey, Edinburgh, UK, ¹⁰Department of Geosciences, Pennsylvania State University, University Park, PA, USA, ¹¹Lunar and Planetary Institute, Houston, TX, USA, ¹²Géosciences Montpellier, Université de Montpellier, Montpellier, France, ¹³Groupe de Physico-Chimie de l'Atmosphère, L'Institut de Chimie et Procédés pour l'Énergie, l'Environnement et la Santé (ICPEES), Université de Strasbourg, Strasbourg, France, ¹⁴Instituto de Geofísica, Universidad Nacional Autónoma de México, Mexico, Mexico, ¹⁵School of Geographical and Earth Sciences, University of Glasgow, Glasgow, UK, ¹⁶Argon Isotope Facility, Scottish Universities Environmental Research Centre, East Kilbride, UK, ¹⁷Department of Geology, University of Freiburg, Freiburg, Germany, ¹⁸Department of Earth Science and Engineering, Imperial College London, London, UK, ¹⁹Department of Geology and Geophysics, University of Utah, Salt Lake City, UT, USA, ²⁰Independent consultant, Cancun, Mexico ²¹Institut für Geologie, Universität Hamburg, Hamburg, Germany, ²²Japan Agency for Marine-Earth Science and Technology, Kanagawa, Japan, ²³Faculty of Earth and Life Sciences (FALW), Vrije Universiteit Amsterdam, Amsterdam, Netherlands, ²⁴Earth and Planetary Sciences, Rutgers University, New Brunswick, NJ, USA, ²⁵Kochi Institute for Core Sample Research, Japan Agency for Marine-Earth Science and Technology, Kochi, Japan, ²⁶Department of Geosciences, University of Alaska Fairbanks, Fairbanks, AK, USA, ²⁷ LeRoy Eyring Center for Solid State Science, Arizona State University, Tempe, AZ, USA, ²⁸School of Earth Sciences, Planetary Science Institute, China University of Geosciences, Wuhan, China, ²⁹Department of Chemistry, Toho University, Chiba, Japan, ³⁰NASA Astrobiology Institute ³¹Aix Marseille Université, CNRS, Institut pour la Recherche et le Développement, Coll France, CEREGE, Aix-en-Provence, France, ³²Centre for Planetary Science and Exploration and Department of Earth Sciences, University of Western Ontario, London, Ontario, Canada

A3. Code and Data Sharing

The SOVA code, as most of the hydrocodes used in impact science, is not currently available for public use. The performance of the code was verified during a special benchmark and validation project (Pierazzo et al., 2008). Raw tracer data (three-dimensional distributions of maximum shock pressure and ejection velocity) are available from the first author upon request. Data used to produce Figures 1 and 2 can be found in Table S1.

Acknowledgments

The European Consortium for Ocean Drilling (ECORD) implemented Expedition 364 with funding from the International Ocean Discovery Program (IODP) and the International Continental scientific Drilling Project (ICDP). Artemieva was supported by NASA grant 15-EXO15_2-0054 and Morgan by NERC grant NE/P005217/1.

References

- Alvarez, L. W., Alvarez, W., Asaro, F., & Michel, H. V. (1980). Extraterrestrial cause of the Cretaceous–Tertiary extinction. *Science*, *208*, 1095–1108.
- Artemieva, N. A. (2017). Ejection of climate active gases after large impacts, *LunarPlanet. Sci. Conf. XLVII*, Abstract 2150.
- Artemieva, N. A., & Morgan, J. V. (2009). Modeling the formation of the K-Pg boundary layer. *Icarus*, *201*, 768–780.
- Artemieva, N. A., Wünnemann, K., Krien, F., Reimold, W. U., & Stöffler, D. (2013). Ries crater and suevite revisited—Observations, modeling Part II: Modeling. *Meteoritics and Planetary Science*, *48*, 590–627.
- Badjukov, D. D., Dikov, Y. P., Petrova, T. L., & Pershin, S. V. (1995). Shock behavior of calcite, anhydrite and gypsum, *Lunar Planetary Science Conference*. XXVI, 63–64.
- Bell, C., Morgan, J. V., Hampson, G. J., & Trudgill, B. (2004). Stratigraphic and sedimentological observations from seismic data across the Chicxulub impact basin. *Meteoritics and Planetary Science*, *39*, 1089–1098. <https://doi.org/10.1111/j.1945-5100.2004.tb01130.x>
- Bell, M. S. (2016). CO₂ release due to impact devolatilization of carbonate: Results of shock experiments. *Meteoritics and Planetary Science*, *51*, 619–646. <https://doi.org/10.1111/maps.12613>
- Belza, J., Goderis, S., Keppens, E., Vanhaeke, F., & Claeys, P. (2012). An emplacement mechanism for the mega-block zone within the Chicxulub impact crater, (Yucatán, Mexico) based on chemostratigraphy. *Meteoritics and Planetary Science*, *47*, 400–413.
- Bourgeois, J., Hansen, T. A., Wiberg, P. L., & Kauffman, E. G. (1988). A tsunami deposit at the Cretaceous-Tertiary boundary in Texas. *Science*, *241*, 567–570.
- Bralower, T. J., Paull, C. K., & Leckie, R. M. (1998). The Cretaceous-Tertiary boundary cocktail: Chicxulub impact triggers margin collapse and extensive sediment gravity flows. *Geology*, *26*, 331–334.
- Brett, R. (1992). The Cretaceous-Tertiary extinction: A lethal mechanism involving anhydrite target rocks. *Geochim Cosmochimica Acta*, *56*, 3603–3606.
- Brugger, J., Feulner, G., & Petri, S. (2017). Baby, it's cold outside: Climate model simulations of the effects of the asteroid impact at the end of the Cretaceous. *Geophysical Research Letters*, *44*, 419–427. <https://doi.org/10.1002/2016GL072241>
- Collins, G. S., Melosh, H. J., & Marcus, R. A. (2005). Earth Impact Effects Program: A Web-based computer program for calculating the regional environmental consequences of a meteoroid impact on Earth. *Meteoritics and Planetary Science*, *40*, 817–840.
- Collins, G. S., Patel, N., Rae, A. S., Davies, T. M., Morgan, J. V., Gulick, S. P. S., & Expedition 364 Scientists (2017). Numerical Simulations of Chicxulub crater formation by oblique impact, *Lunar Planetary Science Conference XLVII*, Abstract 1832.
- D'Hondt, S., Pilon, M. E. Q., Sigurdsson, H., Hanson, A. K., Jr., & Carey, S. (1994). Surface-wateracidification and extinction at the Cretaceous-Tertiary boundary. *Geology*, *22*, 983–986.

- Güldemeister, N., Wünnemann, K., Durr, N., & Hiermaier, S. (2013). Propagation of impact-induced shock waves in porous sandstone using mesoscale modeling. *Meteoritics and Planetary Science*, *48*, 115–133.
- Gulick, S. P. S., Barton, P., Christeson, G. L., Morgan, J. V., McDonald, M., Mendoza-Cervantes, K., ... Warner, M. R. (2008). Importance of pre-impact crustal structure for the asymmetry of the Chicxulub impact crater. *Nature Geoscience*, *1*, 131–135.
- Gupta, S. C., Ahrens, T. J., & Yang, W. (2001). Shock-induced vaporization of anhydrite and global cooling from the K/T impact. *Earth and Planetary Science Letters*, *188*, 399–412.
- Holsapple, K. A., & Housen, K. R. (2007). A crater and its ejecta: An interpretation of deep impact. *Icarus*, *191*, 586–597.
- Ivanov, B. A., & Deutsch, A. (2002). The phase diagram of CaCO₃ in relation to shock compression and decomposition. *Physics of the Earth and Planetary Interiors*, *129*, 131–143.
- Ivanov, B. A., Badukov, D. D., Yakovlev, O. I., Gerasimov, M. V., Dikov, Y. P., Pope, K. O., & Ocampo, A. C. (1996). Degassing of sedimentary rocks due to Chicxulub impact: Hydrocode and physical simulations. In G. Ryder, D. Fastovsky, & S. Gartner (Eds.), *The Cretaceous Tertiary Event and Other Catastrophes in Earth History, Special Papers Geological Society of America* (Vol. 307, pp. 125–139). <https://doi.org/10.1130/0-8137-2307-8.125>
- Kenkmann, T., Wittmann, A., & Scherler, D. (2004). Structure and impact indicators of the Cretaceous sequence of the ICDP drill core Yaxcopoil-1, Chicxulub impact crater, Mexico. *Meteoritics & Planetary Science*, *39*, 1069–1088.
- Kotra, R. K., See, T. H., Gibson, E. K., Hörz, F., Cintala, M. J., & Schmidt, R. S. (1983). Carbon dioxide loss in experimentally shocked calcite and limestone. *Lunar Planetary Science Conference*, XIV, 401–402.
- Kowitz, A., Güldermeister, N., Schmitt, R. T., Reimold, W. U., Wünnemann, K., & Holzwarth, A. (2016). Revision and recalibration of existing shock classifications for quartzose rocks using low-shock pressure (2.5–20 GPa) recovery experiments and mesoscale numerical modeling. *Meteoritics and Planetary Science*, *51*, 1741–1761. <https://doi.org/10.1111/maps.12712>
- Kring, D. A. (2007). The Chicxulub impact event and its environmental consequences at the Cretaceous-Tertiary boundary. *Palaeogeography Palaeoclimatology Palaeoecology*, *255*, 4–21. <https://doi.org/10.1016/j.palaeo.2007.02.037>
- Lange, M. A., & Ahrens, T. J. (1986). Shock-induced CO₂ loss from CaCO₃; implications for early planetary atmospheres. *Earth and Planetary Science Letters*, *77*, 409–418.
- Langenhorst, F., & Deutsch, A. (2012). Shock metamorphism of minerals. *Elements*, *8*, 31–36. <https://doi.org/10.2113/gselements.8.1.31>
- López-Ramos, E. (1975). Geological summary of the Yucatán Peninsula. In A. E. M. Nairn, & F. G. Stehli (Eds.), *Ocean Basins and Margins, the Gulf of Mexico and Caribbean* (pp. 257–282). New York: Plenum Press.
- Martinez, I., Deutsch, A., Schärer, U., Ildefonso, P., Guyot, F., & Agrinier, P. (1995). Shock recovery experiments on dolomite and thermodynamic calculations of impact induced decarbonation. *Journal of Geophysical Research*, *100*, 15,465–15,476. <https://doi.org/10.1029/95JB01151>
- Melosh, H. J. (2007). A hydrocode equation of state for SiO₂. *Meteoritics and Planetary Science*, *42*, 2079–2098.
- Melosh, H. J., Schneider, N. M., Zahnle, K. J., & Latham, D. (1990). Ignition of global wildfires at the Cretaceous-Tertiary boundary. *Nature*, *343*, 251–254.
- Morgan, J., Artemieva, N., & Goldin, T. (2013). Revisiting wildfires at the K-Pg boundary. *Journal of Geophysical Research: Biogeosciences*, *118*, 1508–1520. <https://doi.org/10.1002/2013JG002428>
- Morgan, J. V., & Warner, M. R. (1999). The third dimension of a multi-ring impact basin. *Geology*, *27*, 407–410.
- Morgan, J. V., Gulick, S. P. S., Bralower, T., Chenot, E., Christeson, G., Claeys, Ph., ... Zylberman, W. (2016). The formation of peak rings in large impact craters. *Science*, *354*, 878–882.
- O'Keefe, J. D., & Ahrens, T. J. (1989). Impact production of CO₂ by the Cretaceous/Tertiary extinction bolide and the resultant heating of the Earth. *Nature*, *338*, 247–249. <https://doi.org/10.1038/338247a0>
- Pierazzo, E., Artemieva, N., Asphaug, E., Baldwin, E. C., Cazamias, J., Coker, R., ... Wünnemann, K. (2008). Validation of numerical codes for impact and explosion cratering: Impacts on strengthless and metal targets. *Meteoritics and Planetary Science*, *43*, 1917–1938.
- Pierazzo, E., Artemieva, N. A., & Ivanov, B. A. (2005). Starting conditions for hydrothermal systems underneath Martian craters: Hydrocode modeling. *Geological Society of America Special Papers*, *384*, 443–457.
- Pierazzo, E., Hahmann, A. N., & Sloan, C. (2003). Chicxulub and climate: Radiative perturbations of impact-produced S-bearing gases. *Astrobiology*, *3*, 99–118. <https://doi.org/10.1089/153110703321632453>
- Pierazzo, E., Kring, D. A., & Melosh, H. J. (1998). Hydrocode simulation of the Chicxulub impact event and the production of climatically active gases. *Journal of Geophysical Research*, *103*, 28,607–28,625. <https://doi.org/10.1029/98JE02496>
- Pope, K. O., Baines, K. H., Ocampo, A. C., & Ivanov, B. A. (1994). Impact winter and the Cretaceous/Tertiary extinctions: Results of a Chicxulub asteroid impact model. *Earth and Planetary Science Letters*, *128*, 719–725.
- Prescher, C., Langenhorst, F., Hornemann, U., & Deutsch, A. (2011). Shock experiments on anhydrite and new constraints on the impact-induced SO_x release at the K-Pg boundary. *Meteoritics and Planetary Science*, *46*, 1619–1629.
- Rebolledo-Vieyra, M., & Urrutia-Fucugauchi, J. (2004). Magnetostratigraphy of the impact breccias and post-impact carbonates from borehole Yaxcopoil-1, Chicxulub impact crater, Yucatán, Mexico. *Meteoritics and Planetary Science*, *39*, 821–829.
- Rebolledo-Vieyra, M., & Urrutia-Fucugauchi, J. (2006). Magnetostratigraphy of the Cretaceous/Tertiary boundary and early Paleocene sedimentary sequence from the Chicxulub impact crater. *Earth, Planets and Space*, *58*, 1309–1314. <https://doi.org/10.1186/BF03352626>
- Schulte, P., Deutsch, A., Salge, T., Berndt, J., Kontny, A., MacLeod, K. G., ... Krumm, S. (2009). A dual-layer Chicxulub ejecta sequence with shocked carbonates from the Cretaceous–Paleogene (K–Pg) boundary, Demerara Rise, western Atlantic. *Geochimica et Cosmochimica Acta*, *73*, 1180–1204.
- Schulte, P., et al. (2010). The Chicxulub asteroid impact and mass extinction at the Cretaceous-Paleogene boundary. *Science*, *327*, 1214–1218.
- Shuvalov, V. V. (1999). Multidimensional hydrodynamic code SOVA for interfacial flows: Application to the thermal layer effect. *Shock Waves*, *9*, 381–390.
- Sigurdsson, H., D'Hondt, S., & Carey, S. (1992). The impact of the Cretaceous/Tertiary bolide on evaporite terrain and the generation of major sulfuric acid aerosol. *Earth and Planetary Science Letters*, *109*, 543–559.
- Takata, T., & Ahrens, T. J. (1994). Numerical simulation of impact cratering at Chicxulub and the possible causes of KT catastrophe. In *New developments regarding the KT event and other catastrophes in Earth history, Contribution 825* (pp. 125–126). Houston, TX: Lunar and Planetary Institute.
- Toon, O. B., Pollack, J. P., Ackerman, T. P., Turco, R. P., McKay, C. P., & Liu, M. S. (1982). Evolution of an impact generated dust cloud and its effects on the atmosphere. In L. T. Silver, & P. H. Schultz (Eds.), *Geological Implications of Impacts of Large Asteroids and Comets on the Earth, Special Papers Geological Society of America* (Vol. 190, pp. 187–200).
- Toon, O. B., Zahnle, K., Morrison, D., Turco, R. P., & Covey, C. (1997). Environmental perturbations caused by the impacts of asteroids and comets. *Reviews of Geophysics*, *35*, 41–78. <https://doi.org/10.1111/j.1749-6632.1997.tb48357.x>

- Tyburczy, J. A., & Ahrens, T. J. (1986). Dynamic compression and volatile release of carbonates. *Journal of Geophysical Research*, *91*, 4730–4744. <https://doi.org/10.1029/JB091iB05p04730>
- Ward, S. N., & Asphaug, E. (2000). Asteroid impact tsunamis: A probabilistic hazard assessment. *Icarus*, *145*, 64–78. <https://doi.org/10.1006/icar.1999.6336>
- Wolbach, W. S., Lewis, R. S., & Anders, E. (1985). Cretaceous extinctions: Evidence for wildfires and search for meteoritic material. *Science*, *230*, 167–230. <https://doi.org/10.1126/science.230.4722.167>
- Yang, W., Ahrens, T. J., & Chen, G. (1996). Shock vaporization of anhydrite and calcite and the effect on global climate from K/T impact crater at Chicxulub. *Lunar and Planetary Science*, *XXVII*, 1473–1474.